Neuron
Report

Temporally Precise Cell-Specific Coherence Develops in Corticostriatal Networks during Learning

Aaron C. Koralek,[1] Rui M. Costa,[4] and Jose M. Carmena[1,2,3,*]
[1]Helen Wills Neuroscience Institute
[2]Department of Electrical Engineering and Computer Sciences
[3]Joint Graduate Group in Bioengineering UCB/UCSF
University of California, Berkeley, Berkeley, CA 94720, USA
[4]Champalimaud Neuroscience Programme, Champalimaud Center for the Unknown, 1400-038 Lisbon, Portugal
*Correspondence: jcarmena@berkeley.edu
http://dx.doi.org/10.1016/j.neuron.2013.06.047

SUMMARY

It has been postulated that selective temporal coordination between neurons and development of functional neuronal assemblies are fundamental for brain function and behavior. Still, there is little evidence that functionally relevant coordination emerges preferentially in neuronal assemblies directly controlling behavioral output. We investigated coherence between primary motor cortex and the dorsal striatum as rats learn an abstract operant task. Striking coherence developed between these regions during learning. Interestingly, coherence was selectively increased in cells controlling behavioral output relative to adjacent cells. Furthermore, the temporal offset of these interactions aligned closely with corticostriatal conduction delays, demonstrating highly precise timing. Spikes from either region were followed by a consistent phase in the other, suggesting that network feedback reinforces coherence. Together, these results demonstrate that temporally precise coherence develops during learning specifically in output-relevant neuronal populations and further suggest that correlations in oscillatory activity serve to synchronize widespread brain networks to produce behavior.

INTRODUCTION

For any given task, the nervous system must coordinate the activity of large ensembles of individual neurons across distant brain regions. Even in seemingly trivial motor tasks, such as holding a cup of coffee, large ensembles of neurons must interact to properly control the musculature and monitor sensory feedback. Although the nervous system is equipped with dense anatomical connectivity to support interactions between cell groups, these interactions must be rapidly and flexibly altered as we move from one behavioral context to the next, and particularly as we learn a new skill.

Brain-machine interface (BMI) tasks involve learning to modulate neuronal activity in order to control a disembodied actuator (Fetz, 2007) and therefore provide a completely novel learning environment for subjects. Surprisingly, past work has shown that neuroprosthetic skills rely on similar neural substrates as natural motor learning (Green and Kalaska, 2011) and therefore have similar computational requirements for rapid and flexible information transfer. Importantly, BMI tasks offer the unique advantage that researchers can define which neuronal ensembles are directly relevant for behavioral output, therefore allowing for an investigation of functional specificity within local populations.

Recent theories have proposed that alterations in the pattern of large-scale synchronous activity could serve as the substrate for the flexible neuronal associations necessary to coordinate network activity for performance of both natural and neuroprosthetic behaviors (Womelsdorf et al., 2007; Canolty et al., 2010). Oscillatory local field potential (LFP) activity reflects rhythmic current flow across cell membranes in local ensembles and is hypothesized to alter the excitability of cell groups across different spatiotemporal scales (Buzsáki and Draguhn, 2004; Lakatos et al., 2005; Fröhlich and McCormick, 2010). Therefore, precise temporal control in neural networks could enhance the efficiency of information transfer in specific populations (Wang et al., 2010; Tiesinga et al., 2001). It could also serve as a mechanism for synaptic gain control (Zeitler et al., 2008) and influence spike-timing-dependent plasticity (Huerta and Lisman, 1993; Harris et al., 2003), as spikes arriving at excitability peaks will have enhanced efficacy relative to poorly timed spikes. Temporally coordinated activity in ensembles of neurons has been implicated in processes as diverse as perception (Rodriguez et al., 1999), expectation (von Stein et al., 2000), decision making (Pesaran et al., 2008), coordination (Dean et al., 2012), memory (Pesaran et al., 2002; Siegel et al., 2009), spatial cognition (Colgin et al., 2009), reward processing (van der Meer and Redish, 2011), and attentional shifting (Bollimunta et al., 2011; Lakatos et al., 2008; Fries et al., 2008). In some cases, this synchrony manifests as spiking in one region, becoming highly coordinated with LFP activity in a separate region (Pesaran et al., 2008). Importantly, many tasks evoke changes in the temporal pattern of spiking without concomitant changes in firing rate,

suggesting that synchrony could serve as an additional information channel in neural circuits (Riehle et al., 1997). Alterations in synchrony and LFP dynamics have also been implicated in pathological states such as epilepsy (Bragin et al., 2010) and Parkinson's disease (Costa et al., 2006), highlighting their importance for normal brain functioning.

Despite increasing evidence that changes in synchronous LFP activity are related to changes in behavior during learning (DeCoteau et al., 2007), there is little evidence that temporal coordination emerges selectively in neurons that are controlling behavior. For example, although previous work has demonstrated selectivity of corticomuscular coherence across hemispheres (Schoffelen et al., 2011), there is less evidence of selective coherence emerging in cells directly relevant for behavioral output, largely because the differential participation of neighboring neurons in behavior is difficult to disentangle. In addition, investigating the progression of coherent interactions across learning in individual animals has only recently become possible due to the development of chronically implantable multielectrode arrays. Corticostriatal networks exhibit plasticity during action learning (Costa et al., 2004; Hikosaka et al., 1999), which involves changes in coherence between distal regions (Koralek et al., 2012), and they therefore serve as an important model system for investigating changing interactions across learning. Here, we examine the dynamics and specificity of the temporal interactions between distal nodes of corticostriatal circuits during learning using a BMI paradigm that permits the definition of output-relevant neurons.

RESULTS

Acquisition of a Neuroprosthetic Skill

We developed a BMI task in which rats were required to modulate activity in primary motor cortex (M1) irrespective of physical movements (Figure 1A; Koralek et al., 2012). Modulation of M1 ensemble activity produced changes in the pitch of an auditory cursor, which provided constant auditory feedback to rats about task performance. Reward was delivered when rats precisely modulated M1 activity to move this auditory cursor to one of two target tones, and a trial was marked incorrect if no target had been hit within a 30 s time limit. Two neural ensembles consisting of two to four well-isolated units each were randomly chosen to control the auditory cursor (see Supplemental Experimental Procedures and Figure S1 available online). The action of these ensembles opposed each other, such that increased activity in one ensemble produced increases in cursor pitch, while increased activity in the other ensemble decreased cursor pitch. Thus, in order to achieve a high-pitched target, rodents had to increase activity in the first ensemble and decrease activity in the second, while the opposite modulations were necessary to hit a low-pitched target (Figure 1B). Firing rates were smoothed with a moving average of the past three 200 ms time bins, and rate modulations therefore had to be maintained for a target to be hit. In this sense, the task required rodents to volitionally bring M1 into a desired state irrespective of motor output. Importantly, this task allows us to directly define cells that are relevant for behavioral output and therefore infer the causal link between activity in these cells and behavior.

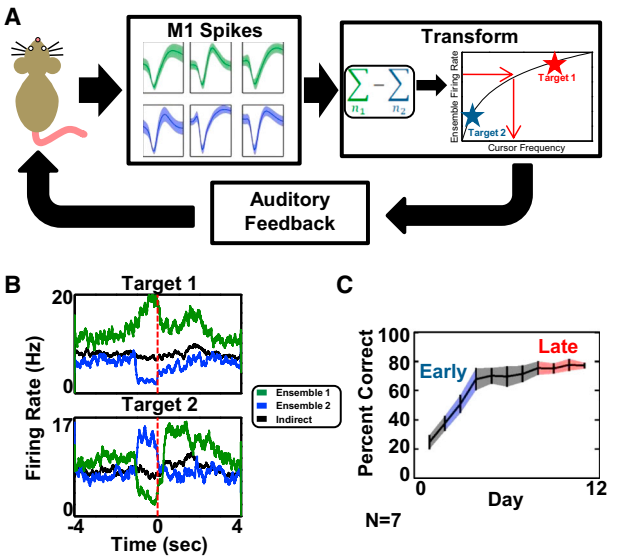

Figure 1. Volitional Modulation of M1 Neural Activity in Awake Behaving Rats

(A) Task schematic. M1 unit activity was entered into an online transform algorithm that related ensemble activity to the pitch of an auditory cursor. Two opposing ensembles were chosen, with activity of one ensemble increasing the cursor pitch and activity of the other ensemble decreasing the cursor pitch. Constant auditory feedback about cursor location was supplied to rodents, and distinct rewards were supplied when rodents brought M1 activity into one of two target states. (B) Mean M1 ensemble firing rates for units in ensemble 1 (green), ensemble 2 (blue), and M1 units not used in the transform (black) in relation to the achievement of target 1 (top) or target 2 (bottom). Time zero indicates target achievement (red dashed line). (C) Mean percentage of correct responses for all rats across days 1–11 of learning. Shaded regions denote the SEM and colored regions denote the range of days from which the early (blue) and late (red) analyses were performed. See also Figure S1.

We chronically implanted a group of rats (n = 8) with microelectrode arrays to simultaneously record activity in both M1 and the dorsal striatum (DS) throughout learning and trained them in this paradigm. A subset of these rats were used in a previous study (Koralek et al., 2012) but underwent additional experimental manipulations for the present work, and two additional rats were used exclusively for this study. The mean percentage of correct trials increased greatly over the course of learning, following a standard learning curve (Figure 1C). There was an initial phase of rapid improvement followed by a phase of slower learning, representing early (days 2–4) and late (days 8–11) learning. The percentage of correct trials increased significantly from early to late in learning ($p < 0.001$), demonstrating that rats were able to properly learn the task. Analyses of M1 firing rates further showed that rats were producing the desired ensemble rate modulations during task performance (Figure 1B).

Corticostriatal Coherence Develops during Neuroprosthetic Learning

We first investigated the relationship between spiking activity and the LFP oscillations recorded during task engagement. We performed spike-triggered averaging of the LFP in late learning

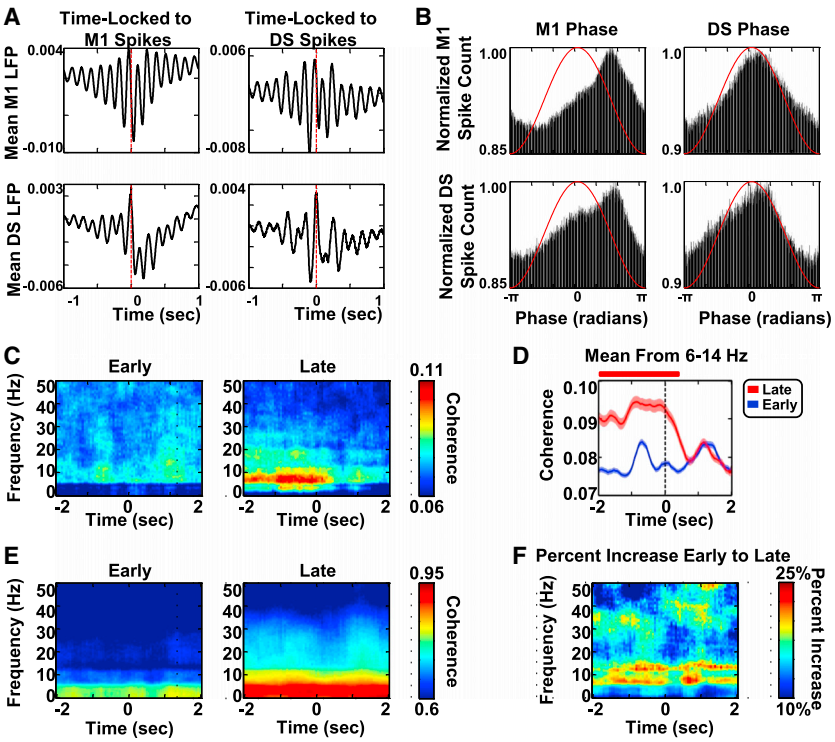

Figure 2. Coherence Develops in Corticostriatal Networks during Learning

(A) The mean M1 LFP (top row) or DS LFP (bottom row) time locked to occurrences of spikes from M1 (left column) or DS (right column). All four average traces exhibit clear LFP oscillations with a strong component at roughly 8 Hz, showing that phase at this frequency influences spiking. (B) Spikes from M1 (top row) or DS (bottom row) fire at a preferred phase of the 6–14 Hz band in the M1 LFP (left column) or DS LFP (right column). (C) Coherograms showing the grand average of coherence between M1 spikes and DS LFP in early (left) and late (right) learning time locked to target achievement. There is a clear increase from early to late in learning, with particularly pronounced activity in the 6–14 Hz band. (D) Mean coherence from 6–14 Hz in early (blue) and late (red) learning time locked to target achievement. Shaded regions denote SEM. Colored bars above plot designate time points with significant differences. (E) Coherograms showing the grand average of coherence between M1 LFP and DS LFP in early (left) and late (right) learning time locked to target achievement. There is a clear increase in low-frequency coherence during learning. (F) Percent increase in coherence from early to late learning shows that this effect is most pronounced in the 6–14 Hz band. See also Figure S2.

time locked to spikes occurring either in the same region or in the other region. If spiking activity was independent of LFP phase, then fluctuations would cancel and produce a flat average LFP. Instead, we observed clear mean LFP oscillations in both regions around action potentials from both regions; this oscillatory activity had a strong component between 6–14 Hz (Figure 2A). This is consistent with past work showing that oscillations in this range are prominent in corticostriatal circuits when performing well-learned tasks (Berke et al., 2004), as well as work suggesting that M1 is predisposed to operate in this frequency range (Castro-Alamancos, 2013). We therefore filtered the raw LFP from 6–14 Hz and calculated the predominant phase at which spikes occurred. Again, we observed clear phase locking of spikes to the ongoing 6–14 Hz LFP in both regions (Figure 2B). Although the relationship between LFP and spiking is certainly complex and cells spike at several preferred LFP phases, there was nevertheless a dominant phase preference across both regions. Interestingly, both DS and M1 spikes occurred preferentially at the peak of the striatal 6–14 Hz LFP oscillation, suggesting that DS firing is maximal at the peak of the DS LFP.

To further quantify these interactions and the ways they evolve during learning, we calculated coherence between spiking activity in M1 and LFP oscillations in DS. We analyzed 1,936 spike-field pairs (121 M1 units and 16 DS LFP channels). To avoid effects of evoked responses on coherence estimates, we subtracted the mean DS event-related potential (ERP) and M1 time-varying firing rate for each cell or LFP channel, respectively, from individual trials before calculating coherence (Figure S2). We saw a profound increase in spike-field coherence across a range of low frequencies in late learning, when rats were skillfully performing the task, relative to early learning (Figure 2C). This effect was most pronounced at frequencies between 6 and 14 Hz and there was a significant increase in mean coherence at these frequencies from early to late in learning (Figure 2D; $p < 0.001$, Bonferroni corrected). However, while subtracting the mean ERP often reduces the effect of evoked potentials on estimates of coherence, it has also been shown that such a procedure can produce artifacts (Truccolo et al., 2002). We therefore repeated the analysis without subtracting the mean ERP and again found a profound increase in 6–14 Hz coherence from early to late learning (Figure S2). This change in coherence was not due to differences in trial number between early and late learning (Figure S2). Importantly, coherence was highest during target reaching and decreased after trial completion at time 0 when the animals initiated movements toward reward. Before trial completion, coherence was significantly higher on correct relative to incorrect trials (Figure S2). In addition, coherence between the M1 LFP and DS LFP also increased from early to late learning (Figure 2E), and this effect was most pronounced between 6 and 14 Hz (Figure 2F). We therefore focused further analyses on this frequency band. These data suggest that corticostriatal ensembles become tightly coordinated over the course of learning.

Coherence Is Specific to Output-Relevant Neurons and to Task Performance

We then asked whether this increase in coherence between M1 spikes and DS LFP was present in all M1 cells recorded or was specific to task-relevant cells. The operant BMI task used here offers the unique advantage that the cells that are directly controlling the output of the BMI (hereafter "output cells"; n = 31)

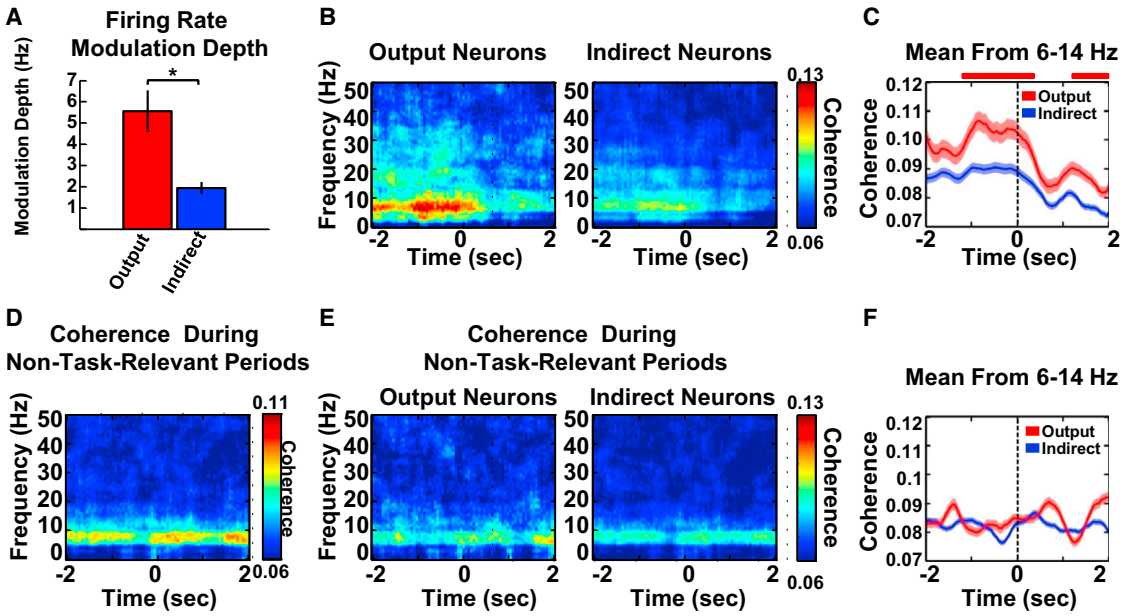

Figure 3. Coherence Is Specific to Task Output-Relevant Neurons and Task-Relevant Time Periods

(A) Firing rate modulation depth for output (red) and indirect (blue) cells in late learning (mean ± SEM). There is significantly greater modulation of output cells relative to indirect cells. (B) Coherograms in late learning showing the grand average for output (left) and indirect cells (right) time locked to target achievement. Coherence is markedly stronger in output than indirect cells. (C) Mean coherence from 6–14 Hz in late learning for output cells (red) and indirect cells (blue) time locked to target achievement. Shaded regions denote SEM. Colored bars above plot designate time points with significant differences. (D) Coherence in late learning is greatly reduced when rats are not actively engaged in the task. Plot shows the grand average across animals. (E) When rats are not performing the task, there is no difference in coherence for output (left) and indirect (right) cells. (F) Mean coherence from 6–14 Hz in late learning when rats are not performing the task again shows no difference between output (red) and indirect (blue) cells. Shaded regions denote SEM. See also Figure S3.

are explicitly defined. Because past work has demonstrated enhanced rate modulations in output cells relative to cells not entered into the BMI (Ganguly et al., 2011; hereafter "indirect cells"; n = 89), we first examined the firing rate modulations that rats produced during task performance. Although indirect cells do not directly impact cursor movement, they are embedded in the same network as output cells and modulation of their activity could therefore still play an indirect role in target achievement. However, in late learning, rats modulated output cells significantly more than indirect cells before target achievement (Figure 3A; $p < 0.001$), suggesting that indirect cells were indeed being treated as less task relevant than output cells. Importantly, we found that the M1-DS coherence that emerged during learning was highly specific to output cells (Figure 3B), even when they were recorded on the same electrode as indirect cells and separated from this population by less than 100 μm. This effect again appeared to be more pronounced in the 6–14 Hz range, with significantly larger coherence in output relative to indirect cells (Figure 3C; $p < 0.01$, Bonferroni corrected). We ensured that well-isolated units were included in both the output and indirect populations, and further verified that these populations did not differ in baseline firing rate (Experimental Procedures and Figure S1). Nevertheless, coherence estimates can be affected by firing rate (Lepage et al., 2011) and the task structure required differences in firing rates in the two populations during target achievement. We therefore performed a thinning procedure to equate firing rates in the two populations (Gregoriou et al., 2009; Experimental Procedures). Despite differences in firing rate being removed, there remained a significant difference in spike-field coherence between output cells and indirect cells (Figure S3; $p < 0.001$, Bonferroni corrected), demonstrating that this effect was not driven by firing rate differences. To further ensure that our results were not affected by firing rate, we separated our analysis by cell and trial type to examine trials in which output cells were required to increase their firing rate to achieve the target and trials in which output cells decreased their firing rate (Figure S3). There was still a significant difference in coherence between output cells that decreased their firing rate relative to indirect cells ($p < 0.05$, Bonferroni corrected), despite no significant difference in firing rate between these populations. Finally, we also calculated coherence after removing cells with low signal-to-noise ratio (SNR) from the indirect population and coherence remained higher in output cells than indirect cells, demonstrating that the effect was not due to differences in SNR (Figure S3; $p < 0.05$, Bonferroni corrected). These coherent interactions were greatly diminished between trials when rats were not actively engaged in the task (Figure 3D). Furthermore, during these periods, the difference in coherence between output and indirect populations was abolished (Figures 3E and 3F). These results show that the corticostriatal coherence that emerged during learning was highly specific for neurons that are directly relevant to behavioral output, even when they are closely intermingled with other cells, and that these precise interactions are flexible and appear rapidly as needed during task performance.

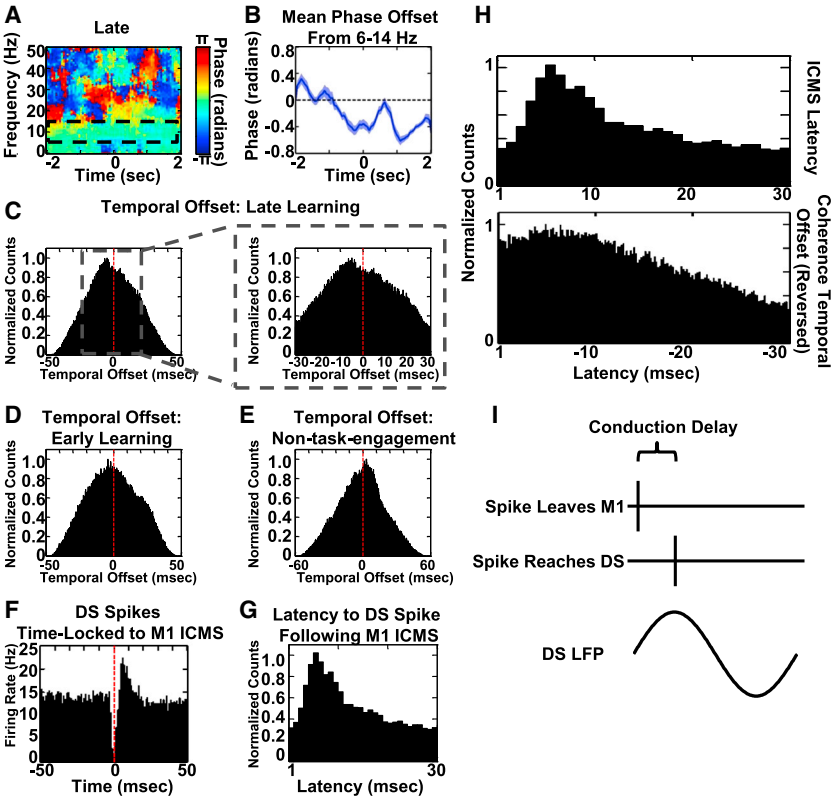

Figure 4. M1 Spikes Are Precisely Timed to the DS LFP during Task Performance

(A) Phase values in late learning show a negative phase in the 6–14 Hz band relative to other frequency ranges. By convention, this suggests that M1 spikes lead the DS LFP. (B) The mean phase from 6–14 Hz surrounding target achievement exhibiting consistently negative phase. Shaded region denotes SEM. (C) The distribution of temporal offset estimates obtained from the coherence phase data for every trial and every spike-field pair (see Experimental Procedures) shows that M1 spikes most often occur 5–7 ms before the peak of the DS 6–14 Hz LFP. (D) The distribution of temporal offset estimates in early learning does not show the same phase preference seen in late learning. (E) The distribution of temporal offset estimates in late learning when rats were not actively engaged in the task does not show the same phase preference seen during task engagement. (F) Mean spiking response in the DS time locked to application of ICMS to M1. (G) Histogram of the latency to DS spikes after application of ICMS to M1 as a measure of the corticostriatal conduction delay. There is a clear peak 5–7 ms after application of ICMS. (H) The ICMS-based estimate of the conduction delay (top) aligns remarkably well with temporal offset estimates from the spike-field coherence analysis (bottom). Temporal offsets are plotted with a reversed x axis to correspond with the ICMS results. (I) A working model for our results. M1 spikes precede the DS LFP 6–14 Hz band peak by 5–7 ms, which is on scale with the corticostriatal conduction delay. Thus, after accounting for this delay, M1 spikes arrive at the DS during peak excitability. See also Figure S4.

Precise Timing of Corticostriatal Activity

Because we found that M1 spikes occurred preferentially at the peak of the DS LFP (Figure 2B), we next investigated the phase offset of the spike-field coherence. From the mean phase heat map, we see that there is a consistent negative phase offset in the 6–14 Hz range (Figure 4A). By convention, this suggests that M1 spikes precede the peak of the DS LFP in the 6–14 Hz band. Indeed, the phase at 6–14 Hz was commonly negative, as can be seen in the distribution of phase offsets for every cell and every frequency from 6 to 14 Hz (Figure 4B). When phase offset values are used to estimate a temporal delay between M1 spikes and DS LFP (see Experimental Procedures), we see a clear preference for M1 cells to fire at an offset of −5 to −7 ms relative to the DS LFP, as reflected in the mode of this distribution (Figure 4C; SEM = 0.03 ms). This preference developed over the course of training and was not present in early stages of learning (Figure 4D) or in late learning when rats were not actively engaged in the task (Figure 4E), suggesting that it is not innately apparent in corticostriatal circuits. In addition, this temporal offset was specific to the 6–14 Hz band (Figure S4). These results show that M1 is on average spiking 6 ms before the peak of the DS LFP when rats are performing a well-learned task.

The DS receives strong input from M1, and this temporal offset is concordant with past estimates of the conduction delay between these regions (Cowan and Wilson, 1994), suggesting that M1 input may be driving DS firing (which occurs preferentially at the peak of the DS LFP). We therefore applied intracortical microstimulation (ICMS) to M1 while recording responses in DS and estimated the delay between M1 ICMS and DS response. Brief cathodal pulses were applied to M1 and produced a consistent spiking response in the DS (Figure S4 and Experimental Procedures). We performed 3,245 ICMS trials in seven animals over several sessions. The mean peristimulus time histogram (PSTH) time locked to ICMS shows a marked peak in DS spiking following application of ICMS to M1 (Figure 4F). For every cell, we then estimated the corticostriatal conduction delay by calculating the latency from M1 stimulation until the first DS spike occurred (Figure 4G). This distribution of latencies had a mode at 6 ms (SEM = 0.1 ms), which is on scale with past estimates of the conduction delay (Vandermaelen and Kitai, 1980). There was striking alignment between this estimate of the conduction delay and the temporal offset determined above, and these distributions were not significantly different from each other (Figure 4H, $p = 0.45$). Together, these results suggest that M1 spikes in late learning are precisely timed to drive DS during task performance (Figure 4I).

Network Activity Drives the 6–14 Hz LFP Oscillation

Our finding of a consistent nonzero phase lag concordant with the conduction delay between the two regions suggests that the regions may interact directly rather than being coordinated by a third region. To further investigate a mechanism for these precise dynamics, we calculated spike-triggered phase

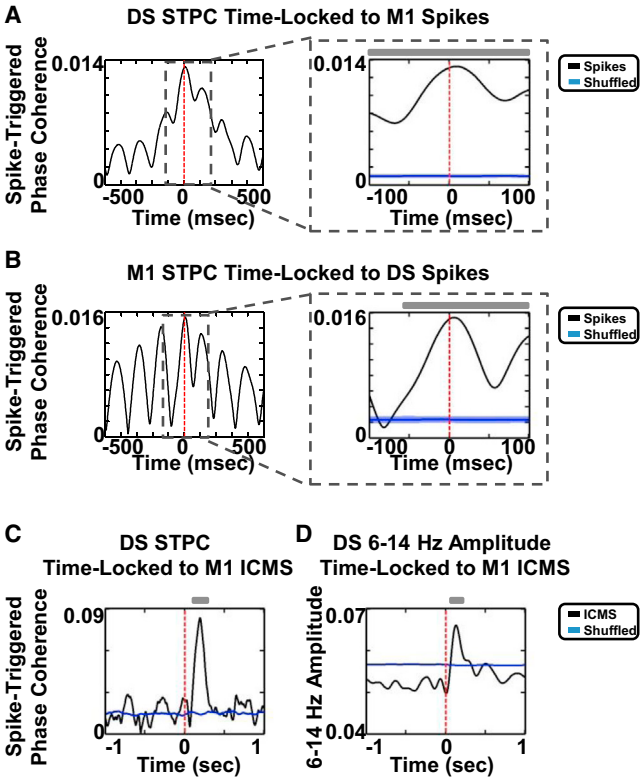

Figure 5. Intertrial Phase Coherence Suggests Entrainment of the LFP by Network Spikes during Task Engagement

Colored bars above all plots denote time points with significant differences and shaded regions denote SEM. (A) DS 6–14 Hz STPC time locked to M1 spikes exhibits a marked peak immediately following M1 activity. DS STPC (black) is significantly greater than the distribution of 6,000 STPC values obtained by shuffling the timing of recorded spikes (blue). (B) M1 6–14 Hz STPC time locked to DS spikes also exhibits a clear peak following DS activity. M1 STPC (black) is significantly greater than surrogate STPC values (blue). (C) DS 6–14 Hz STPC (black) time locked to application of ICMS to M1. ICMS in M1 is followed by a consistent phase in the DS. This is significantly greater than surrogate STPC values (blue). (D) DS 6–14 Hz amplitude time locked to application of ICMS to M1 (black). ICMS in M1 is followed by an increase in 6–14 Hz amplitude in the DS. This peak is significantly greater than values obtained on a surrogate data set (blue). See also Figure S5.

coherence (STPC) in the 6–14 Hz band of both regions time locked to spikes from either region (Experimental Procedures). STPC measures phase consistency from spike to spike. This measure will be 1 if, at a given time point, the phase is the same surrounding every spike, and it will be 0 if the phase is random. By investigating the time course of coherence surrounding a spike, the STPC measure is suggestive of the direction of influence between spikes and LFP, although it cannot conclusively rule out the influence of a third region. Importantly, the DS STPC exhibited a pronounced peak after spikes from M1 are fired, showing that M1 spikes are followed by a consistent phase in the DS (Figure 5A; $p < 0.001$, Bonferroni corrected). Interestingly, we found a similar effect for the reverse calculation, with STPC in M1 significantly enhanced following spikes from the DS (Figure 5B; $p < 0.001$, Bonferroni corrected). This shows that activity in the DS is followed by a consistent phase in M1 and underscores that corticostriatal circuits function as re-entrant loops. To investigate whether M1 activity caused the 6–14 Hz activity or simply coordinated ongoing activity, we also calculated STPC in the DS surrounding application of ICMS to M1 (Figure 5C) and found that STPC was significantly enhanced after M1 ICMS ($p < 0.001$, Bonferroni corrected), suggesting that strong ICMS-induced activity in M1 produces entrainment that drives the DS 6–14 Hz oscillation. These peaks in STPC are significantly greater than values obtained with surrogate data sets in which spike or event times are shuffled (Experimental Procedures). Importantly, M1 ICMS is also followed by an enhancement of 6–14 Hz amplitude in the DS (Figure 5D; $p < 0.001$, Bonferroni corrected), suggesting that strong M1 activity drives the 6–14 Hz activity in the DS rather than coordinating ongoing activity. Interestingly, the peak in 6–14 Hz amplitude following ICMS precedes the peak in STPC. This amplitude peak is again greater than values obtained with surrogate data sets. Together, these data suggest that, after learning, spiking in M1 or DS produces a consistent LFP phase in the other region, resulting in reinforcement of coherent dynamics throughout the network.

DISCUSSION

In summary, we have shown that coherence develops in corticostriatal networks during learning with high temporal precision and, importantly, specifically involving cells that control behavioral output, even when these cells are intermingled with other neuronal populations. This specificity suggests that coherence can serve to enhance communication between task-relevant populations and bias local competitive interactions in their favor. This, in turn, allows for rapid modulation of the functional connectivity between local ensembles and distant brain structures and for flexible routing of specific signals throughout the brain as these signals become immediately relevant for behavior. Interestingly, this cell-specific coherence occurred predominantly in the alpha band, between 6 and 14 Hz. This is consistent with recent work showing low-frequency coherence between M1 spikes and DS spikes (Koralek et al., 2012). The slight shift in frequency between spike-spike and spike-field coherence in the same task may reflect that spike-spike coherence measures similarity between output spike trains, while spike-field coherence measures similarity between the output of one region and synchronous input to another (Zeitler et al., 2006). Differences between these measures in the dominant frequency of coherence could therefore reflect individual neurons not spiking on every cycle of the population rhythm or performing temporal integration of inputs.

A number of distinct rhythms have been previously observed in this frequency range. While some of these rhythms, such as high-voltage spindles or mu rhythms, are thought to be generated in thalamocortical circuits (Hughes and Crunelli, 2005), other forms of 6–14 Hz LFP activity in M1 are thought to be generated via local circuit mechanisms (Castro-Alamancos, 2013). Importantly, sleep spindles in this frequency range have been associated with memory consolidation (Steriade and Timofeev, 2003). In addition, alpha band activity in the visual system (Kandel and Buzsáki, 1997) and mu rhythms in the sensorimotor

system (Nicolelis et al., 1995), both centered roughly at 6–14 Hz, are associated with disengagement from external stimuli. Thus, our finding of enhanced phase locking of M1 spikes to the DS alpha band LFP in late learning could reflect the rats learning to disengage the corticostriatal system from the musculature in order to perform our neuroprosthetic task.

In addition, the precise timing of neuronal inputs that we observed could have consequences for network dynamics and plasticity throughout the brain. A large body of work has shown that temporal precision modulates the induction and direction of long-lasting synaptic plasticity (Dan and Poo, 2004). Indeed, computational models have demonstrated the importance of timing for spike-timing-dependent plasticity and information transfer in neuronal networks (Wang et al., 2010). Input timing is particularly important for the regulation of dendritic calcium levels in striatal cells and, in turn, synaptic plasticity (Kerr and Plenz, 2004). Thus, the precise temporal dynamics demonstrated here may have important functional consequences for corticostriatal plasticity and its role in learning.

Our results also suggest the intriguing possibility that these precise temporal interactions can be maintained by activity within the network reinforcing synchronous LFP oscillations. Corticobasal ganglia circuits are organized as closed feedback loops (Hikosaka et al., 1999), with activity in any node influencing the flow of information through the system. Our finding of enhanced STPC following spikes in either M1 or DS therefore suggests that this flow of feedback through re-entrant corticostriatal loops maintains the orderliness and strength of coherence in the system. Indeed, while past work has suggested that oscillations spanning a range of frequencies are produced in the thalamus, removal of corticothalamic feedback by decortication results in disordered oscillations (Contreras et al., 1996), highlighting the importance of network feedback mechanisms in the control and organization of coherent activity.

In summary, our data support coherence as an effective means by which functional cell assemblies can quickly form and disband to meet task demands, as well as demonstrating ways in which such neuronal interactions can be learned and adapted to support a lifetime of flexible, skilled behavior.

EXPERIMENTAL PROCEDURES

See Supplemental Experimental Procedures for details.

SUPPLEMENTAL INFORMATION

Supplemental Information includes Supplemental Experimental Procedures and five figures and can be found with this article online at http://dx.doi.org/10.1016/j.neuron.2013.06.047.

ACKNOWLEDGMENTS

We thank J.D. Long II for technical support and R.T. Canolty for helpful discussion. This work was supported by the National Science Foundation CAREER Award 0954243, the Multiscale Systems Research Center, and the Defense Advanced Research Projects Agency contract N66001-10-C-2008 to J.M.C., and the International Early Career Scientists Grant from the Howard Hughes Medical Institute, the Marie Curie International Reintegration Grant 239527, and European Research Council STG 243393 to R.M.C.

Accepted: June 27, 2013
Published: August 15, 2013

REFERENCES

Berke, J.D., Okatan, M., Skurski, J., and Eichenbaum, H.B. (2004). Oscillatory entrainment of striatal neurons in freely moving rats. Neuron *43*, 883–896.

Bollimunta, A., Mo, J., Schroeder, C.E., and Ding, M. (2011). Neuronal mechanisms and attentional modulation of corticothalamic α oscillations. J. Neurosci. *31*, 4935–4943.

Bragin, A., Engel, J., Jr., and Staba, R.J. (2010). High-frequency oscillations in epileptic brain. Curr. Opin. Neurol. *23*, 151–156.

Buzsáki, G., and Draguhn, A. (2004). Neuronal oscillations in cortical networks. Science *304*, 1926–1929.

Canolty, R.T., Ganguly, K., Kennerley, S.W., Cadieu, C.F., Koepsell, K., Wallis, J.D., and Carmena, J.M. (2010). Oscillatory phase coupling coordinates anatomically dispersed functional cell assemblies. Proc. Natl. Acad. Sci. USA *107*, 17356–17361.

Castro-Alamancos, M.A. (2013). The motor cortex: a network tuned to 7-14 Hz. Front Neural Circuits *7*, 21, http://dx.doi.org/10.3389/fncir.2013.00021.

Colgin, L.L., Denninger, T., Fyhn, M., Hafting, T., Bonnevie, T., Jensen, O., Moser, M.B., and Moser, E.I. (2009). Frequency of gamma oscillations routes flow of information in the hippocampus. Nature *462*, 353–357.

Contreras, D., Destexhe, A., Sejnowski, T.J., and Steriade, M. (1996). Control of spatiotemporal coherence of a thalamic oscillation by corticothalamic feedback. Science *274*, 771–774.

Costa, R.M., Cohen, D., and Nicolelis, M.A. (2004). Differential corticostriatal plasticity during fast and slow motor skill learning in mice. Curr. Biol. *14*, 1124–1134.

Costa, R.M., Lin, S.C., Sotnikova, T.D., Cyr, M., Gainetdinov, R.R., Caron, M.G., and Nicolelis, M.A. (2006). Rapid alterations in corticostriatal ensemble coordination during acute dopamine-dependent motor dysfunction. Neuron *52*, 359–369.

Cowan, R.L., and Wilson, C.J. (1994). Spontaneous firing patterns and axonal projections of single corticostriatal neurons in the rat medial agranular cortex. J. Neurophysiol. *71*, 17–32.

Dan, Y., and Poo, M.-M. (2004). Spike timing-dependent plasticity of neural circuits. Neuron *44*, 23–30.

Dean, H.L., Hagan, M.A., and Pesaran, B. (2012). Only coherent spiking in posterior parietal cortex coordinates looking and reaching. Neuron *73*, 829–841.

DeCoteau, W.E., Thorn, C., Gibson, D.J., Courtemanche, R., Mitra, P., Kubota, Y., and Graybiel, A.M. (2007). Learning-related coordination of striatal and hippocampal theta rhythms during acquisition of a procedural maze task. Proc. Natl. Acad. Sci. USA *104*, 5644–5649.

Fetz, E.E. (2007). Volitional control of neural activity: implications for brain-computer interfaces. J. Physiol. *579*, 571–579.

Fries, P., Womelsdorf, T., Oostenveld, R., and Desimone, R. (2008). The effects of visual stimulation and selective visual attention on rhythmic neuronal synchronization in macaque area V4. J. Neurosci. *28*, 4823–4835.

Fröhlich, F., and McCormick, D.A. (2010). Endogenous electric fields may guide neocortical network activity. Neuron *67*, 129–143.

Ganguly, K., Dimitrov, D.F., Wallis, J.D., and Carmena, J.M. (2011). Reversible large-scale modification of cortical networks during neuroprosthetic control. Nat. Neurosci. *14*, 662–667.

Green, A.M., and Kalaska, J.F. (2011). Learning to move machines with the mind. Trends Neurosci. *34*, 61–75.

Gregoriou, G.G., Gotts, S.J., Zhou, H., and Desimone, R. (2009). High-frequency, long-range coupling between prefrontal and visual cortex during attention. Science *324*, 1207–1210.

Harris, K.D., Csicsvari, J., Hirase, H., Dragoi, G., and Buzsáki, G. (2003). Organization of cell assemblies in the hippocampus. Nature *424*, 552–556.

Hikosaka, O., Nakahara, H., Rand, M.K., Sakai, K., Lu, X., Nakamura, K., Miyachi, S., and Doya, K. (1999). Parallel neural networks for learning sequential procedures. Trends Neurosci. *22*, 464–471.

Huerta, P.T., and Lisman, J.E. (1993). Heightened synaptic plasticity of hippocampal CA1 neurons during a cholinergically induced rhythmic state. Nature *364*, 723–725.

Hughes, S.W., and Crunelli, V. (2005). Thalamic mechanisms of EEG alpha rhythms and their pathological implications. Neuroscientist *11*, 357–372.

Kandel, A., and Buzsáki, G. (1997). Cellular-synaptic generation of sleep spindles, spike-and-wave discharges, and evoked thalamocortical responses in the neocortex of the rat. J. Neurosci. *17*, 6783–6797.

Kerr, J.N.D., and Plenz, D. (2004). Action potential timing determines dendritic calcium during striatal up-states. J. Neurosci. *24*, 877–885.

Koralek, A.C., Jin, X., Long, J.D., 2nd, Costa, R.M., and Carmena, J.M. (2012). Corticostriatal plasticity is necessary for learning intentional neuroprosthetic skills. Nature *483*, 331–335.

Lakatos, P., Shah, A.S., Knuth, K.H., Ulbert, I., Karmos, G., and Schroeder, C.E. (2005). An oscillatory hierarchy controlling neuronal excitability and stimulus processing in the auditory cortex. J. Neurophysiol. *94*, 1904–1911.

Lakatos, P., Karmos, G., Mehta, A.D., Ulbert, I., and Schroeder, C.E. (2008). Entrainment of neuronal oscillations as a mechanism of attentional selection. Science *320*, 110–113.

Lepage, K.Q., Kramer, M.A., and Eden, U.T. (2011). The dependence of spike field coherence on expected intensity. Neural Comput. *23*, 2209–2241.

Nicolelis, M.A., Baccala, L.A., Lin, R.C., and Chapin, J.K. (1995). Sensorimotor encoding by synchronous neural ensemble activity at multiple levels of the somatosensory system. Science *268*, 1353–1358.

Pesaran, B., Pezaris, J.S., Sahani, M., Mitra, P.P., and Andersen, R.A. (2002). Temporal structure in neuronal activity during working memory in macaque parietal cortex. Nat. Neurosci. *5*, 805–811.

Pesaran, B., Nelson, M.J., and Andersen, R.A. (2008). Free choice activates a decision circuit between frontal and parietal cortex. Nature *453*, 406–409.

Riehle, A., Grün, S., Diesmann, M., and Aertsen, A. (1997). Spike synchronization and rate modulation differentially involved in motor cortical function. Science *278*, 1950–1953.

Rodriguez, E., George, N., Lachaux, J.P., Martinerie, J., Renault, B., and Varela, F.J. (1999). Perception's shadow: long-distance synchronization of human brain activity. Nature *397*, 430–433.

Schoffelen, J.-M., Poort, J., Oostenveld, R., and Fries, P. (2011). Selective movement preparation is subserved by selective increases in corticomuscular gamma-band coherence. J. Neurosci. *31*, 6750–6758.

Siegel, M., Warden, M.R., and Miller, E.K. (2009). Phase-dependent neuronal coding of objects in short-term memory. Proc. Natl. Acad. Sci. USA *106*, 21341–21346.

Steriade, M., and Timofeev, I. (2003). Neuronal plasticity in thalamocortical networks during sleep and waking oscillations. Neuron *37*, 563–576.

Tiesinga, P.H.E., Fellous, J.-M., Jose, J.V., and Sejnowski, T.J. (2001). Optimal information transfer in synchronized neocortical neurons. Neurocomputing *38–40*, 397–402.

Truccolo, W.A., Ding, M., Knuth, K.H., Nakamura, R., and Bressler, S.L. (2002). Trial-to-trial variability of cortical evoked responses: implications for the analysis of functional connectivity. Clin. Neurophysiol. *113*, 206–226.

van der Meer, M.A.A., and Redish, A.D. (2011). Theta phase precession in rat ventral striatum links place and reward information. J. Neurosci. *31*, 2843–2854.

Vandermaelen, C.P., and Kitai, S.T. (1980). Intracellular analysis of synaptic potentials in rat neostriatum following stimulation of the cerebral cortex, thalamus, and substantia nigra. Brain Res. Bull. *5*, 725–733.

von Stein, A., Chiang, C., and König, P. (2000). Top-down processing mediated by interareal synchronization. Proc. Natl. Acad. Sci. USA *97*, 14748–14753.

Wang, H.-P., Spencer, D., Fellous, J.-M., and Sejnowski, T.J. (2010). Synchrony of thalamocortical inputs maximizes cortical reliability. Science *328*, 106–109.

Womelsdorf, T., Schoffelen, J.-M., Oostenveld, R., Singer, W., Desimone, R., Engel, A.K., and Fries, P. (2007). Modulation of neuronal interactions through neuronal synchronization. Science *316*, 1609–1612.

Zeitler, M., Fries, P., and Gielen, S. (2006). Assessing neuronal coherence with single-unit, multi-unit, and local field potentials. Neural Comput. *18*, 2256–2281.

Zeitler, M., Fries, P., and Gielen, S. (2008). Biased competition through variations in amplitude of gamma-oscillations. J. Comput. Neurosci. *25*, 89–107.